Diffusing assumptions in astroparticle physics

M Sarkis[1] and G Beck[1]

[1] Department of Physics, University of the Witwatersrand, Private Bag 3, WITS-2050, Johannesburg, South Africa

E-mail: michael.sarkis@students.wits.ac.za

Abstract. Previous calculations of diffuse synchrotron radio emissions from dark matter annihilations have made use of a semi-analytical solution method for the diffusive cosmic ray transport equation. This method requires that various halo properties like the magnetic field and thermal gas density are spatially independent. We evaluate the physical accuracy of this approximation by calculating the expected synchrotron flux from three astrophysical sources, the Coma galaxy cluster, the M33 galaxy and the Reticulum II dwarf spheroidal galaxy. We find that for large structures, where diffusion effects are less significant to the output flux, using an average weighted with the dark matter halo density for magnetic field and gas density profiles results in a lower observed flux. We note that prescription is more accurate to the physical scenario than the conventionally used unweighted average and indicates that results dependent on such averages may be optimistic. Additionally, we explore other common approximations and detail their effects.

1. Introduction

There have been many studies in the literature that calculate the expected radio emissions from dark matter (DM) residing in astronomical structures. These studies typically calculate the synchrotron flux from secondary electrons, produced by DM annihilations, with the goal of constraining various DM properties via radio observations. For a review of these methods, see [1, 2, 3] and references therein. With the MeerKAT project and the upcoming Square Kilometre Array in mind, this important avenue of DM hunting will likely play an even larger role in future indirect DM detection studies.

A rigorous calculation of the radio emissions from DM secondary electrons involves the solution of a general cosmic-ray transport equation with diffusion and energy loss effects, which is a second-order partial differential equation that depends on the spatial structure of the host environment. Several simplifying assumptions have thus been utilised by authors when studying these radio emissions in order to find a tractable and analytic solution. One of the assumptions commonly used in the literature is that the magnetic field permeating the host DM halo is spatially independent. This form allows one to find a semi-analytical formula for the solution to the diffusive transport equation, allaying the need for full numerical methods. Since real magnetic fields in large structures will have some kind of spatial dependence, this assumption is generally carried out in two separate ways. The first is to take a simple spatial average of an assumed/observed magnetic field profile, and the second is to assume a constant or 'flat' magnetic field strength throughout the entire region of interest. Another assumption that could be made to drastically simplify the calculation of the synchrotron flux is that diffusion effects

can be neglected altogether, and that the synchrotron flux is determined entirely by the peak energy of the emission, leading to the so-called monochromatic approximation.

Here we aim to evaluate the impact of some of these assumptions on the observed flux from various astronomical sources ranging from dwarf spheroidal galaxies (dSphs) to galaxy clusters. To do this, we calculate the synchrotron flux for three astronomical targets using a variety of often-used assumptions and approximations.

2. Halo and DM particle models

2.1. Halo properties

The formulation of halo properties in this work closely resembles that of [4]. For any further details, we therefore refer the reader to [4] and references therein. We consider two density profiles, the NFW [5] and Einasto [6], to characterise the DM halos in the targets considered here. These profiles are given as:

$$\rho_{\rm NFW}(r) = \frac{\rho_{\rm s}}{\frac{r}{r_{\rm s}}\left(1+\frac{r}{r_{\rm s}}\right)^2}\,, \qquad \rho_{\rm Ein}(r) = \rho_{\rm s}\exp\left[-\frac{2}{\alpha}\left(\left[\frac{r}{r_{\rm s}}\right]^{\alpha}-1\right)\right] \tag{1}$$

where $r_{\rm s}$ and $\rho_{\rm s}$ are the halo scale radius and density respectively, and α is the Einasto parameter. The thermal gas density ($n_{\rm e}$) and magnetic field (B) are chosen to have the following profiles:

$$n_{\rm e,PL}(r) = n_0 \quad 1+\left[\frac{r}{r_{\rm d}}\right]^2\Bigg)^{-q_e}, \qquad B_{\rm PL}(r) = B_0\left(\frac{n_{\rm e}(r)}{n_0}\right)^{q_{\rm b}} \tag{2}$$

$$n_{\rm e,Exp}(r) = n_0\exp\left(-\frac{r}{r_{\rm d}}\right), \qquad B_{\rm Exp}(r) = B_0\exp\left(-\frac{r}{r_{\rm d}}\right) \tag{3}$$

where $q_{\rm e} = 1.125$, $q_{\rm b} = 0.5$, as in [4]. A list of properties for the DM density, magnetic field and thermal gas profiles of each source target is shown in Table 1.

Table 1: List of astronomical source targets and their halo properties.

Target name	ρ_χ profile	$n_{\rm e}(r)$ profile	$B(r)$ profile	$n_0\,({\rm cm}^{-3})$	$B_0\,(\mu{\rm G})$	$r_{\rm d}\,({\rm kpc})$
Coma	NFW	PL	PL	3.44×10^{-3}	4.7	290.0
M33	NFW	Exp	Exp	0.03	13.34	5.0
Reticulum II	Ein ($\alpha = 0.4$)	Exp	Exp	1.0×10^{-6}	$\sim$1.0	0.015

2.2. Spatial dependence of magnetic field and thermal gas density

When analytically solving for the electron equilibrium distribution with the transport equation (see Equation 5 below), a common simplifying assumption made in the literature is that the diffusion and energy loss coefficients have no spatial dependence. Since this assumption requires a spatially independent magnetic field and thermal gas density, simple 'flat' averages of these quantities have been used – notably in the code package RX-DMFIT [7] (see also [8, 9] and references therein). Since the rate of annihilation of WIMPs is strongly dependent on the density profile of the halo, as in [4] we consider a weighted average for the magnetic field or thermal gas density that uses the squared DM density of the halo as a tracer for the regions in the halo that have a more significant impact on the total observed flux. This weighting factor is taken from the dependence of the annihilation particle source function (see Equation 4 below) on halo density. We argue that this is a more realistic modelling scenario than a flat average over the entire halo, which takes into equal account those regions in which there may be very little or negligible contributions to the overall flux (typically in the outer edges of the halo).

2.3. Particle Source function

The annihilation of WIMPs inside a DM halo is expected to lead to the production of a set of kinematically-accessible SM products. The following particle source function,

$$Q(E,r) = \frac{1}{2}\langle\sigma v\rangle \sum_f \frac{\mathrm{d}N_\mathrm{e}^f}{\mathrm{d}E} B_f \left(\frac{\rho_\chi(r)}{m_\chi}\right)^2 , \tag{4}$$

describes the distribution of particles formed by a single annihilation. Here $\langle\sigma v\rangle$ is the velocity-averaged annihilation cross-section, $\mathrm{d}N_\mathrm{e}^f/\mathrm{d}E$ is the particle energy spectrum (obtained from [10]), B_f is the branching ratio for the channel indexed by f and m_χ is the WIMP mass. In this work, as is common in indirect DM detection studies, we consider each channel individually and set B_f to 1 for each channel of interest. We also only consider a representative WIMP mass of $m_\chi = 100$ GeV, as we are studying environmental effects that will not scale with WIMP mass.

3. Radio emissions from DM annihilation

The electrons and positrons produced by WIMP annihilations are expected to interact with magnetic fields and the thermal electron population within the halo environment. The radiative and cooling effects are usually encapsulated in a transport equation, here given by

$$\frac{\partial}{\partial t}\frac{\mathrm{d}n_\mathrm{e}}{\mathrm{d}E} = \nabla\cdot\left(D(E,\mathbf{x})\nabla\frac{\mathrm{d}n_\mathrm{e}}{\mathrm{d}E}\right) + \frac{\partial}{\partial E}\left(b(E,\mathbf{x})\frac{\mathrm{d}n_\mathrm{e}}{\mathrm{d}E}\right) + Q_\mathrm{e}(E,\mathbf{x}) , \tag{5}$$

where $D(E,\mathbf{x})$ and $b(E,\mathbf{x})$ are the diffusion and energy loss coefficients respectively, and would in general depend on the position $\mathbf{x}$ within the halo. In this work we take these to be:

$$D(E) = D_0 \left(\frac{d_0}{1\,\mathrm{kpc}}\right)^{\frac{2}{3}} \left(\frac{\langle B\rangle}{1\,\mu\mathrm{G}}\right)^{-\frac{1}{3}} \left(\frac{E}{1\,\mathrm{GeV}}\right)^{\frac{1}{3}} , \tag{6}$$

and

$$b(E) = b_\mathrm{IC}\left(\frac{E}{1\,\mathrm{GeV}}\right)^2 + b_\mathrm{synch}\left(\frac{E}{1\,\mathrm{GeV}}\right)^2\langle B\rangle^2 + b_\mathrm{coul}\langle n_\mathrm{e}\rangle\left(1+\frac{1}{75}\log\left(\frac{\gamma}{\langle n_\mathrm{e}\rangle}\right)\right) + b_\mathrm{brem}\langle n_\mathrm{e}\rangle\left(\frac{E}{1\,\mathrm{GeV}}\right) . \tag{7}$$

Here D_0 is the diffusion constant, d_0 is the magnetic field coherence length, γ is the electron Lorentz factor, and b_IC, b_synch, b_coul and b_brem are the energy loss coefficients for Inverse Compton, synchrotron, Coulomb scattering and bremsstrahlung effects. As in [4], we use the following values for each in units of 10^{-16} GeV s^{-1}, respectively: 0.25, 0.0254, 6.13, 4.7. The quantities $\langle B\rangle$ and $\langle n_\mathrm{e}\rangle$ are calculated by the description in Section 2.2.

The solution of Equation 5 can be found via the semi-analytic method described in [8]. If the DM halo and thermal electron population are considered spherically symmetric and the diffusion and energy loss coefficients are spatially independent, the equilibrium electron distribution is

$$\frac{\mathrm{d}n_\mathrm{e}}{\mathrm{d}E}(r,E) = \frac{1}{b(E)}\int_E^{m_\chi} \mathrm{d}E' G(r,E,E') Q(r,E') , \tag{8}$$

where $G(r,E,E')$ is a Green's function. For the full derivation of this solution, and details about the form of this function, we refer the reader to [8].

The average power of synchrotron radiation produced by electrons/positrons with energy E and at a redshift z, at an observed frequency of ν, is then calculated using the following equation [11]:

$$P_\mathrm{synch}(\nu,E,r,z) = \int_0^\pi \mathrm{d}\theta \frac{\sin\theta^2}{2} 2\pi\sqrt{3} r_\mathrm{e} m_\mathrm{e} c \nu_\mathrm{g} F_\mathrm{synch}\left(\frac{\kappa}{\sin\theta}\right) . \tag{9}$$

 ISBN: 978-0-620-97693-0

Here $m_{\rm e}$, $r_{\rm e} = e^2/m_{\rm e}c^2$ and $\nu_{\rm g} = eB/2\pi m_{\rm e}c$ are the mass, classical radius and gyro-radius of an electron respectively. The value of κ is given by

$$\kappa = \frac{2\nu(1+z)}{3\nu_{\rm g}\gamma^2}\left[1+\left(\frac{\gamma\nu_{\rm p}}{\nu(1+z)}\right)^2\right]^{3/2}, \tag{10}$$

where $\nu_{\rm p} \propto \sqrt{n_{\rm e}}$ is the plasma frequency, and the synchrotron kernel function $F_{\rm synch}(x)$ is calculated with

$$F_{\rm synch}(x) = x\int_x^\infty {\rm d}y K_{5/3}(y) \approx 1.25x^{1/3}{\rm e}^{-x}(648+x^2)^{1/12}. \tag{11}$$

Combining the average power emitted per electron/positron in Equation 9 with the equilibrium spectral distribution of electrons/positrons, we finally calculate the synchrotron flux at frequency ν to a target at a luminosity distance of $D_{\rm L}$ as

$$S(\nu,z) = \frac{1}{4\pi D_{\rm L}^2}\int_0^r\int_{m_{\rm e}}^{m_\chi} {\rm d}^3r'\,{\rm d}E\left(\frac{{\rm d}n_{\rm e^-}}{{\rm d}E}+\frac{{\rm d}n_{\rm e^+}}{{\rm d}E}\right)P_{\rm synch}(\nu,E,r',z)\,, \tag{12}$$

where ${\rm d}n_{\rm e^{-,+}}/{\rm d}E$ are the equilibrium spectral distributions of electrons, positrons respectively.

3.1. Monochromatic approximation

If we assume a simplifying monochromatic form for the synchrotron kernel function [1, 3, 12], *i.e.* that the peak electron energy corresponds to the frequency of the emitted radiation, then $F_{\rm synch}(x) \sim \delta(x - 0.29)$ and the peak energy can be determined by $E(\nu) \simeq 0.463\ \nu^{1/2}\ B^{-1/2}$ GeV, with the frequency ν in Mhz and the magnetic field strength B in μG. Under the additional assumption of a constant magnetic field strength B, the synchrotron flux can then simply be approximated using the formula

$$S_{mono}(\nu) \approx \frac{1}{4\pi D_{\rm L}^2}\left[\frac{9\sqrt{3}\langle\sigma v\rangle}{2m_\chi^2(1+C)}E(\nu)Y(\nu,m_\chi)\int {\rm d}^3x\rho_\chi({\bf x})^2\right], \tag{13}$$

where $Y(\nu,m_\chi) = \int_{E(\nu)}^{m_\chi}{\rm d}E'(dN_{\rm e}/dE')$ (and $dN_{\rm e}/dE$ is the particle energy spectrum from Equation 4) and C is the ratio of synchrotron to Inverse Compton scattering energy loss coefficients.

4. Results and discussion

We have calculated and plotted the fluxes from three source targets using various approximate formulae, including different forms for the magnetic field and gas density, and in the case of the Coma galaxy cluster, different synchrotron flux equations. These are shown in Figure 1, which shows the results for the Coma galaxy cluster (top), the M33 galaxy (bottom-left) and Reticulum II dSph (bottom-right). In each plot we have shown the flux, $S(\nu)$, for the case of a radially-dependent magnetic field profile, $B(r)$, that has been spatially averaged with both flat and ρ_χ^2 weights. We also show fluxes calculated with a flat magnetic field profile that has a strength $B_{\rm x}$, with the subscript denoting the value in μG in each case. We consider WIMPs of mass 100 GeV that annihilate entirely into the $b\bar{b}$ channel, and assume a thermal relic annihilation cross section of $\langle\sigma v\rangle = 3.0\times10^{-26}{\rm cm}^3\,{\rm s}^{-1}$.

In the Coma galaxy cluster we first note that diffusion effects, represented by the dashed curves, are almost negligible. This is an expected feature of fluxes calculated for large structures like galaxy clusters where diffusion timescales are small compared to other energy-loss

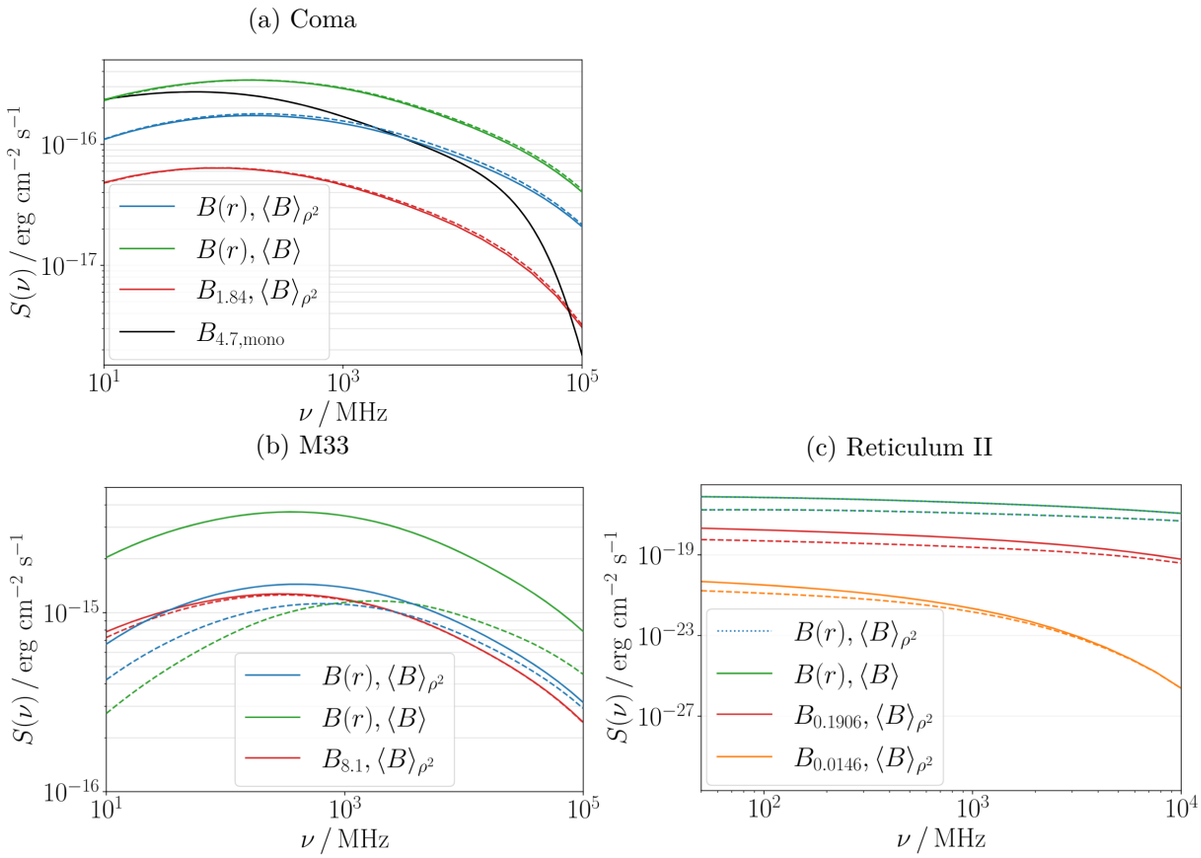

Figure 1: Expected radio synchrotron flux output from (a): the Coma galaxy cluster, (b): the M33 galaxy and (c): the Reticulum II dSph. Each solid curve represents a calculation with a different treatment of halo parameters (see text) and without diffusion effects. The dashed curves of each colour show the same calculation with diffusion included in the calculation.

mechanisms (for a detailed analysis of diffusion in galaxy clusters, we refer the reader to [8]). Using a ρ^2 weighted average for the spatially dependent functions results in a flux that is roughly a factor of 2 lower than using a flat average, and using a flat magnetic field profile further lowers the output flux by roughly a factor of 6. For all targets, we see that the flux output from a flat magnetic field profile is highly dependent on the strength of the field, which highlights the importance of accuracy when choosing this value. In this source we have also calculated the flux using the monochromatic approximation, given by Equation 13. The flux obtained with this calculation has a very steep drop-off at higher frequencies, which may lead to an unnecessary over-emphasis on low frequency data sets. This is caused by the dependence of the flux on the peak frequency and the assumption of a monochromatic synchrotron kernel function. We also note that this approximation does not account for diffusion effects within the halo, which could motivate its use in galaxy cluster approximations but not in smaller structures wherein diffusion effects are generally more significant.

In the M33 galaxy, we see that the inclusion of diffusion effects in the case of an unweighted magnetic field can reduce the output flux by a factor of ~ 1.5 at higher frequencies, and up to a factor of ~ 7.5 at lower frequencies. In the case of a weighted magnetic field, diffusion effects still reduce the expected flux by up to a factor of ~ 1.5 at lower frequencies. The significance of diffusion in these results contrasts with the formulation of radio flux models in [13, 12], where

the flux from the M33 (and M31) galaxy is found from the monochromatic approximation which neglects diffusion completely.

In the Reticulum II dSph, we firstly note that the use of a flat or ρ^2 weighted average for a spatially dependent magnetic field has no discernible effect on the output flux. This could be explained by the relatively small size of the dSph DM halo, which equalises the two averaging techniques. However, we see that the flux has a very strong dependence on the magnetic field strength under the assumption of a flat profile. In the cases shown here, for two values of the magnetic field strength calculated using a flat and weighted average of a fully spatially dependent profile (0.0146 and 0.1906 μG respectively), we see a relative difference of at least 2 orders of magnitude, which increases drastically with higher frequencies. Since this value is typically calculated using an unweighted average of a full magnetic field profile, its use in radio flux approximations may lead to significant uncertainties – especially for smaller structures like the dSph modelled here.

5. Conclusion

We have found that the various assumptions used when calculating the radio synchrotron flux from astronomical DM can have a significant effect on the expected flux from these sources. In particular, we see that the use of flat magnetic field profiles can drastically alter the output flux, especially in the case of smaller structures like the Reticulum II dSph. We also note that the inclusion of diffusion effects in M33, neglected in previous studies, can lead to a noticeable reduction in the expected flux. For larger structures like the Coma galaxy cluster, we find that using a spatial average of the magnetic field weighted with the DM density – which should provide a more realistic estimate of the rate of DM annihilations in different regions of the halo – results in a flux that is lower than when using a flat average by a factor of ~ 2. With the upcoming boost in radio observation capabilities with MeerKAT and the SKA, the assumptions used when hunting for DM with radio synchrotron fluxes should be evaluated carefully for each source target and host environment in order to maximise accuracy.

Acknowledgments

This work is based on the research that was supported by the National Research Foundation of South Africa (Bursary No. 112332). G.B acknowledges support from a National Research Foundation of South Africa Thuthuka grant no. 117969.

References

[1] Profumo S and Ullio P 2010 *Particle Dark Matter: Observations, Models and Searches* (Cambridge, UK: Cambridge University Press)
[2] Beck G 2019 *Galaxies* **7**
[3] Chan M H 2019 *Galaxies* **9** 11
[4] Beck G 2021 *JCAP* **2021** 007
[5] Navarro J, Frenk C and White S 1997 *ApJ* **490** 493–508
[6] Einasto J 1968 *Publications of the Tartuskoj Astrofizica Observatory* **36** 414–41
[7] McDaniel A, Jeltema T, Profumo S and Storm E 2017 *JCAP* **2017** 027
[8] Colafrancesco S, Profumo S and Ullio P 2006 *A & A* **455** 21–43
[9] Colafrancesco S, Marchegiani P and Beck G 2015 *JCAP* **2015** 032
[10] Cirelli M, Corcella G, Hektor A *et al.* 2011 *JCAP* **2011** 051
[11] Longair M 1994 *High Energy Astrophysics* (Cambridge, UK: Cambridge University Press)
[12] Chan M H, Cui L, Liu J and Leung C S 2019 *ApJ* **872** 177
[13] Chan M H 2017 *Phys. Rev. D* **96**(4) 043009